PCCP

Accepted Manuscript

ROYAL SOCIETY OF CHEMISTRY

www.rsc.org/pccp

Cite this: DOI: 10.1039/x0xx00000x

Are thermodynamic cycles necessary for continuum solvent calculation of p*K*as and reduction potentials?

Junming Ho[a,b]

Received ooth January 2012,
Accepted ooth January 2012

DOI: 10.1039/x0xx00000x

www.rsc.org/

Continuum solvent calculations of p*K*as and reduction potentials usually entail the use of a thermodynamic cycle to express the reaction free energy in terms of gas phase energies and free energies of solvation. In this work, we present a systematic study comparing the solution phase free energy changes obtained in this manner with that directly computed within the SMD solvation model against a large test set of 117 p*K*as and 42 reduction potentials in water and DMSO. The inclusion of vibrational contributions in the free energy of solvation has negligible impact on the accuracy of thermodynamic cycle predictions of p*K*as and reduction potentials. Additionally, when gas phase energies in the thermodynamic cycle are computed at more accurate levels of theory, very similar results (mean unsigned difference of 0.5 kcal mol^{-1}) can be achieved when the high level computations (MP2/GTMP2Large and G3(MP2)-RAD(+)) are directly carried out within the continuum model. Increasing the accuracy of the electronic structure theory may or may not improve the agreement with experiment suggesting that the error is largely in the solvation model. For amino acids where their gas and solution phase species exist as different tautomers, the direct approach provided a significant improvement in calculated p*K*as. These results demonstrate that direct calculation of solution phase p*K*as and reduction potentials within the SMD model provides a general and reliable approximation to corresponding thermodynamic cycle based protocols, and is recommended for systems where solvation induced changes in geometry are significant. Further studies are necessary to ascertain whether the results are generalisable to other continuum solvation models.

1. Introduction

The introduction of computationally efficient continuum solvation models[1-4] (also known as implicit solvation models) marks an important development towards first-principles studies of reactions in the liquid phase. These models have been parameterised to predict the free energies of solvation of common neutral and ionic solutes that can be combined with experimental or *ab initio* gas phase energies for estimating free energy changes in solution. Such procedures have been widely applied in the computation of kinetic and thermodynamic properties such as rate coefficients,[5] p*K*as[6] and reduction potentials[7] in various solvents. These topics have also been extensively reviewed in several recent review articles.[8-12]

Most continuum models adopt the functional form of the free energy of solvation shown in eqn (1),[1] where Ψ^{pol} is the solute wave function, H^0 is the gas phase Hamiltonian and V is the potential energy operator associated with the reaction field. The first term is associated with electrostatics, whilst the second term contains non-electrostatic contributions (dispersion-repulsion and solvent structural terms) to the solvation energy. When the solvation terms and the gas phase electronic energy in eqn (1) are evaluated on geometries optimised in the respective phases, the continuum solvation free energy also includes the effect of geometrical relaxation associated with solvation. Continuum solvation models differ from one another in the manner in which V is constructed, and their treatment of non-electrostatic components. Examples of commonly used solvation models include the polarizable continuum model (PCM) family of methods (e.g. IEF-PCM,[13] CPCM,[14, 15] and IPCM),[16] the SM*x* series (e.g. $x = 8$,[17] D[18]), the IEF-MST model,[19, 20] SS(V)PE model,[21, 22] Poisson-Boltzmann/Jaguar model,[23] and the COSMO-RS method.[24-26]

$$\Delta G_{\text{S}} = \left\langle \Psi^{\text{pol}} \middle| H^{o} + \frac{V}{2} \middle| \Psi^{\text{pol}} \right\rangle + G_{\text{nes}} - E_{\text{gas}} \qquad (1)$$

Recent assessment studies have estimated that the accuracy of continuum solvent calculations of *aqueous* p*K*as and reduction potentials lies in the range of 2-3 units[11] and 250-300 mV[10, 27] respectively. These deviations are still high compared to experimental measurements and there is significant interest towards developing procedures with improved accuracy. The errors in these calculations originate primarily from the solvation contribution since continuum hydration free energies of monovalent ions have relatively large mean errors of at least 4 kcal mol^{-1}.[28, 29] This is due in part to the intrinsic uncertainties in experimental hydration free energies of charged species,[30] and the difficulty of modelling ionic solvation via a dielectric continuum model. In principle, these errors can be mitigated through hybrid cluster-continuum schemes, whereby first solvent shell interactions are treated explicitly at the quantum mechanical level, and the rest of the solvent is approximated by

a dielectric continuum. Examples of such methods include the quasichemical theory of solvation,[31-33] the relaxed cluster-continuum COSMO (rCCC) model,[34] and mixed cluster-continuum schemes.[35, 36] As discussed in a recent review,[30] the performance of cluster-continuum schemes also depends critically on the choice of electronic structure method, solvation model, and proper statistical sampling of the configuration phase space of the ion-solvent cluster.

Recently, there is growing interest towards direct computation of solution phase reaction energies within continuum solvation models, thereby circumventing separate computations of gas phase and solvation free energies. A number of studies[37-41] have considered the use of ideal gas molecular partition functions in conjunction with the rigid rotor harmonic oscillator (RRHO) approximation for computing solution phase reaction free energies within a dielectric continuum solvation model – see eqn (2). The corresponding expression for the gas phase Gibbs free energy of a solute is shown in eqn (3), and $G_{\text{corr}}^{\text{gas}}$ and $G_{\text{corr}}^{\text{soln}}$ are the thermal corrections to the Gibbs free energy (including electronic, translational, rotational, and vibrational contributions) computed in the gas phase and dielectric continuum respectively.

$$G_{\text{soln}}^{*} = \left\langle \Psi^{\text{pol}} \middle| H^{0} + \frac{V}{2} \middle| \Psi^{\text{pol}} \right\rangle + G_{\text{nes}} + G_{\text{soln}}^{\text{corr}} \quad (2)$$

$$G_{\text{gas}}^{*} = E_{\text{gas}} + G_{\text{gas}}^{\text{corr}} \quad (3)$$

$$\Delta G_{\text{S}}^{*} = G_{\text{soln}}^{*} - G_{\text{gas}}^{*} \quad (4)$$

Free energies of solvation computed via eqns (1) and (4) therefore differ by the change in the thermal contribution to the free energy upon solvation ($G_{\text{soln}}^{corr} - G_{\text{gas}}^{corr}$). The validity of this approach has recently been questioned,[42] since the solute is unlikely to behave as an ideal gas in the solution-phase, and therefore the solution phase free energy computed by eqn (2) in conjunction with gas phase partition functions is likely to introduce errors. Additionally, any non-cancelling differences in the thermal correction to the free energies in the gas and solution phase are already incorporated into the continuum model via parameterisation (e.g. definition of atomic radii) to reproduce experimental free energies of solvation. As such, explicit inclusion of thermal corrections to the free energies of solvation, even if the use of gas phase partition functions is valid, is likely incur some degree of double-counting. Notably, for a dataset of 50 neutral and ionic solutes there is a two-fold increase in mean absolute deviations when the PCM-UAHF free energies of solvation are computed via eqn (4) compared to eqn (1).[42]

In a separate study focusing on the SMD solvation model,[44] Cramer and Truhlar clarified that the translational partition function in the gas phase becomes the liberational free energy in solution,[43] and therefore this contribution cancels out in the solvation free energy (eqn (4)) irrespective of whether the solute behaves as an ideal gas in the solution phase. The SMD model has also been parameterised to a dataset composed of small rigid solutes such that the vibrational contribution to the free energy of solvation is largely conserved upon solvation, and that the contributions associated with the conversion of gas phase rotational modes to librational modes in solution are included in the parameterisation of the cavity–dispersion–solvent-structure (CDS) terms in the SM*x* series of continuum models.[44] The authors further reasoned that the sum of the first two terms in eqn (1) is the solution phase analogue of the gas phase potential energy surface (or potential of mean force), and harmonic vibrational corrections computed within the continuum model are valid. Free energies of solvation computed using eqn (4) therefore contains vibrational corrections ($G_{\text{corr}}^{\text{soln}} - G_{\text{corr}}^{\text{gas}}$) that are not included in eqn (1), and is recommended for systems where solvation induced changes in vibrational frequencies are significant. The contrasting behaviour of the PCM-UAHF and SMD models is presumably a consequence of the different manner in which these models have been parameterised and implemented. As such, assumptions concerning the appropriateness of the continuum model vibrational corrections may not be readily transferable to other solvation models, and would need to be validated through further benchmarking studies.

Accordingly, eqn (2) provides an alternative to thermodynamic cycles for assembling a solution phase free energy within the SMD dielectric continuum model. Importantly, the solution phase reaction energies obtained in this manner do not depend *directly* on the accuracy of continuum solvation free energies (in contrast to thermodynamic cycles), and might therefore offer an improvement in accuracy. Several studies have explored free energies obtained in this fashion in conjunction with an *isodesmic* scheme to predict the aqueous p*K*as of a dataset of common organic acids[45-48] and ligands[39, 40] with accuracies that are comparable to corresponding thermodynamic cycle calculations. These results signify the ability of the isodesmic scheme to largely cancel the errors (if any) associated with the free energies calculated via eqn (2). However, there is presently no direct comparison of this approach with corresponding thermodynamic cycle based protocols for the computation of solution phase energetics, and how it performs more broadly for the computation of *general* p*K*as and reduction potentials in aqueous and non-aqueous solvents. Additionally, because continuum solvation models have been parameterised at relatively modest levels of theory (e.g. HF or DFT with a double zeta basis set), it is also unclear as to whether the free energies directly computed using the empirically optimised cavities can be systematically improved through the use of higher levels of theory.

To this end, this study aims to address the following questions: (a) Does the inclusion of vibrational corrections in continuum free energies of solvation improve the accuracy of calculated p*K*as and reduction potentials? (b) How do solution phase reaction energies computed directly within a continuum model compare with corresponding thermodynamic cycle calculation? (c) Are the free energies computed in a dielectric continuum amenable to systematic improvement through the

use of higher levels of electronic structure theory? In the present work, we address these questions using a large database of 117 p*K*as and 42 reduction potentials in water and DMSO to benchmark our theoretical calculations. The SMD solvation model[18] is chosen for this study on the basis of an earlier work justifying the use of solution phase vibrational frequencies in this continuum model,[44] and that it has been designed to predict free energies of solvation in aqueous as well as non-aqueous solvents. It is envisaged that the outcome of this study would provide a better understanding of the scope and limitations associated with direct calculation of solution phase free energies within the framework of continuum solvation models.

2. Theory

Shown in Figure 1 are two thermodynamic cycles commonly used for calculating p*K*as and reduction potentials. The dissociation free energy associated with cycle A is shown in eqn (5).

$$\Delta G^*_{\text{soln}} = \Delta G^*_{\text{gas}} + \Delta G^*_{\text{S}}(\text{H}^+) + \Delta G^*_{\text{S}}(\text{A}^-) - \Delta G^*_{\text{S}}(\text{HA}) \quad (5a)$$

$$\Delta \text{G}^*_{\text{gas}} = G^{\text{o}}_{\text{gas}}(\text{H}^+) + G^{\text{o}}_{\text{gas}}(\text{A}^-) - G^{\text{o}}_{\text{gas}}(\text{HA}) + RT\ln\left(\frac{RT}{P}\right) \quad (5b)$$

The superscripts "*" and "°" denote that the thermochemical quantities are computed with respect to a standard state of 1 mol L^{-1} and 1 atm respectively. The last term in eqn (5b) is a standard state correction.

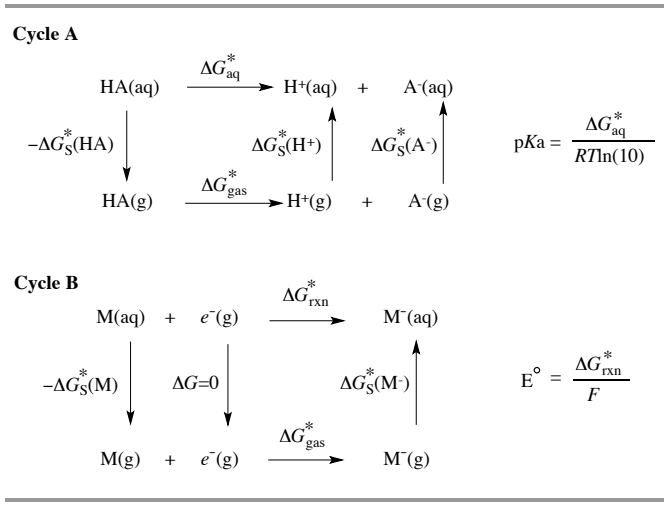

Figure 1. Examples of thermodynamic cycles used for computing p*K*as and reduction potentials.

When the solvation free energies in eqn (5a) are computed using eqn (1), and when all terms in the thermodynamic cycle (gas phase energies and thermal correction as well as solvation free energies) are calculated at the same level of theory, the resulting dissociation free energy becomes:

$$\Delta G^*_{\text{soln}} = E_{\text{soln}}(\text{A}^-) - E_{\text{soln}}(\text{HA}) + G^{\text{gas}}_{\text{corr}}(\text{A}^-) - G^{\text{gas}}_{\text{corr}}(\text{HA}) + G^*_{\text{soln}}(\text{H}^+) \quad (6a)$$

$$\Delta G^*_{\text{soln}} = \Delta E_{\text{soln}} + \Delta G^{\text{gas}}_{\text{corr}} + G^*_{\text{soln}}(\text{H}^+) \quad (6b)$$

$$E_{\text{soln}} = \left\langle \Psi^{\text{pol}} \middle| H^0 + \frac{V}{2} \middle| \Psi^{\text{pol}} \right\rangle + G_{\text{nes}} \quad (6c)$$

where $G^*_{\text{soln}}(\text{H}^+)$ is the solution phase free energy of the proton and $\Delta G^{\text{gas}}_{\text{corr}}$ is thermal contribution to the reaction free energy in the *gas phase*. E_{soln} is the solution phase analogue of the gas phase potential energy, also known as the potential of mean force.[44, 49] The solution phase and gas phase components of the free energy of solvation in eqn (1) are evaluated on the geometry optimised in the respective phases so that the effect of geometrical relaxation is also included.

The principal reason for using a thermodynamic cycle is that continuum solvation models are parameterised to produce accurate free energies of solvation, and the low levels of theory at which they are typically implemented (HF or DFT with a small basis set) are usually not sufficiently accurate to reproduce accurate solution phase free energies. By using a thermodynamic cycle, one can make use of high-level *ab initio* calculations in the gas phase to improve the accuracy of the resulting reaction energies. This usually involves carrying out high level single point calculations on geometries optimised at the lower level theory (e.g. HF or DFT and a double zeta basis set) that are typically implemented for continuum solvation models. The resulting reaction energy expression is shown in eqn (7) where ΔE^X_{gas} is the gas phase reaction energy, and X=H or L denotes energies computed at the high or low level of theory respectively.

$$\Delta G^*_{\text{soln}}(\text{TC}) = \Delta E^{\text{L}}_{\text{soln}} + \Delta G^{\text{gas,L}}_{\text{corr}} + G^*_{\text{soln}}(\text{H}^+) + \Delta E^{\text{H}}_{\text{gas}} - \Delta E^{\text{L}}_{\text{gas}} \quad (7a)$$

$$\Delta E^{\text{X}}_{\text{gas}} = E^{\text{X}}_{\text{gas}}(\text{A}^-) - E^{\text{X}}_{\text{gas}}(\text{HA}) \quad (7b)$$

The corresponding expression for the dissociation free energy using vibrationally-corrected free energies of solvation (eqn (4)) is shown in eqn (8). Thus, the difference between the two dissociation energies lies in the *phase* in which the thermal correction to reaction Gibbs free energy is computed (eqn (9)). As discussed in more detail below, this difference is generally very small (averaging about 0.5 kcal mol^{-1} or less).

$$\Delta G^*_{\text{soln}}(\text{TC}) = \Delta E^{\text{L}}_{\text{soln}} + \Delta G^{\text{soln,L}}_{\text{corr}} + G^*_{\text{soln}}(\text{H}^+) + \Delta E^{\text{H}}_{\text{gas}} - \Delta E^{\text{L}}_{\text{gas}} \quad (8)$$

$$\Delta\Delta G^*_{\text{soln}} = \Delta G^{\text{gas}}_{\text{corr}} - \Delta G^{\text{soln}}_{\text{corr}} \quad (9)$$

It is worth noting that when all the terms in eqn (8) are evaluated at the *same* level of theory (i.e. L=H), the resulting solution phase reaction energies is the same as that directly computed within a continuum solvation model at that level of theory. In other words, the solution phase free energy is *exactly identical* to what would be obtained from an optimisation-frequency calculation in a continuum solvation model. The question that follows is therefore whether one can similarly improve the accuracy of solution phase reaction energies

directly computed within a dielectric continuum model through the use of higher levels of theory:

$$\Delta G^{*}_{\mathrm{soln}} = \Delta E^{\mathrm{H}}_{\mathrm{soln}} + \Delta G^{\mathrm{soln,L}}_{\mathrm{corr}} + G^{*}_{\mathrm{soln}}(\mathrm{H}^{+}) \quad (10)$$

Note that the difference between the reaction energy obtained in this manner and from the corresponding thermodynamic cycle (eqn (8)) is simply the difference in the high level correction to the reaction energy computed in the gas phase and dielectric continuum on geometries optimised in the respective phases.

$$\Delta\Delta G^{*}_{\mathrm{soln}} = (\Delta E^{\mathrm{H}}_{\mathrm{gas}} - \Delta E^{\mathrm{L}}_{\mathrm{gas}})//\mathrm{gas} - (\Delta E^{\mathrm{H}}_{\mathrm{soln}} - \Delta E^{\mathrm{L}}_{\mathrm{soln}})//\mathrm{soln} \quad (11)$$

In the study that follows, we first examine how the inclusion of vibrational contributions in free energies of solvation affects the accuracy of calculated p*K*as and reduction potentials. The next section compares the p*K*as and reduction potentials obtained via a thermodynamic cycle, and calculated directly within the SMD model. High level single point calculations are performed at the MP2/GTMP2Large and the G3(MP2)-RAD(+) level and the resulting solution phase p*K*as and *E*° are compared with experiment. For the benchmarking study, we have compiled a large dataset of 117 p*K*as in water and DMSO, and 42 standard reduction potentials in water. In the last section of this paper, we also examine the performance of both approaches towards the aqueous p*K*a calculation of amino acids where their solution phase and gas phase geometries differ appreciably.

3. Computational details

All electronic structure calculations were carried out using the Gaussian09 program.[50] The test set of molecules and their starting geometries were adopted from refs 10, 11, 51. For the test set of amino acids, systematic conformer searches were carried out in both the gas and solution phase to locate the global minimum energy structure of each species. The gas phase calculations (geometries, electronic energies and thermal corrections to the Gibbs energy) were carried out at the M06-2X/6-31+G(d) level[52] with ultrafine grid. All thermal corrections to the Gibbs free energy were computed using the ideal gas molecular partition functions in conjunction with the rigid-rotor quasiharmonic oscillator (RR-QHO) approximation. In the QHO approximation,[44] vibrational frequencies that were lower than 100 cm^{-1} were raised to 100 cm^{-1} due to the breakdown of the harmonic oscillator model for low frequency vibrational modes. Single-point calculations at the (RO)MP2/GTMP2Large and G3(MP2)-RAD(+) levels of theory were performed on the M06-2X/6-31+G(d) optimised geometries. The G3(MP2)-RAD(+) is a modified version of the G3(MP2)-RAD procedure[53] whereby calculations involving the 6-31G(d) basis set were replaced with the 6-31+G(d) basis set so as to provide an improved description of anionic species. The solution phase calculations were carried in an analogous fashion within the SMD solvation model[18] using the default settings in Gaussian09.[50]

In the p*K*a calculations we have employed the proton free energy $\Delta G^{*}_{\mathrm{S}}(\mathrm{H}^{+})$ of -265.9,[54, 55] -273.3[56] and -260.0[56] kcal mol^{-1} in water, dimethylsulfoxide and acetonitrile respectively, that are consistent with the parameterisation of the SMD model. The gas phase proton free energy $G^{\circ}_{\mathrm{gas}}(\mathrm{H}^{+})$ of -6.3 kcal mol^{-1} have been employed for the gas phase calculations.[57] It should be stressed that the frequency calculations carried out in the gas phase as well as within the SMD model are based on the default standard state in Gaussian09 which is 1 atm and 298.15 K, and appropriate standard state corrections have been applied to ensure that all solution phase p*K*as and reduction potentials are computed at a standard state of 1 mol L^{-1}.

For the calculation of reduction potentials, the value of -0.86 kcal mol^{-1} for the gas phase energy of the electron based on the Fermi-Dirac statistical formalism is employed.[10, 58] As discussed elsewhere,[10, 59] when computing reduction potentials, it is important that one uses a reference value of the standard hydrogen electrode in conjunction with a continuum solvation model that is based on a consistent value of $\Delta G^{*}_{\mathrm{S}}(\mathrm{H}^{+})$. The value of E°_{SHE} 4.28 V used in this work is derived from the aqueous proton solvation free energy that is based on the same thermochemical convention for the electron.[60]

4. Results and Discussion

4.1 Use of vibrationally-corrected free energies of solvation

Table 1 compares the dissociation and reduction free energies employing free energies of solvation computed with and without the inclusion of rovibrational corrections, based on the thermodynamic cycles shown in Figure 1. All high level single point calculations were carried out at the G3(MP2)-RAD(+) level on the M06-2X/6-31+G(d) gas phase geometries. The complete data is provided in Tables S1-S3 in the Supporting Information.

As seen from Table 1, the mean absolute deviations between the two sets of dissociation and reduction free energies $\Delta\Delta G^{*}_{\mathrm{soln}}$ are generally very small (below 0.5 kcal mol^{-1}), and that the maximum absolute deviation is about 2.0 kcal mol^{-1}. The deviation arises from the difference in the thermal correction to the Gibbs free energy calculated in the gas phase and dielectric continuum as shown in eqn (9). The two acids accounting for the largest deviations in $\Delta\Delta G^{*}_{\mathrm{soln}}$ are protonated guanidine (2.0 kcal mol^{-1} in water) and thiourea (1.8 kcal mol^{-1} in DMSO). Closer inspection reveals that the amine groups in both molecules are twisted out of plane in the gas phase, but becomes planar in the solution phase. As shown in Figure 2, this change in geometry is sufficient to alter some of the vibrational modes to introduce significant changes to the vibrational contribution to the free energy of dissociation. By comparison, the rotational contribution is generally very small (< 0.1 kcal mol^{-1}) across the entire test set. Aliphatic alcohols were also observed to display relatively large vibrational corrections (*ca.* 1.7 kcal mol^{-1}), whilst the corresponding values

for their fluorinated and phenolic analogues are at least three times smaller. For these systems, the higher deviations arose as a result of changes in the zero-point vibrational energy associated with the conjugate base of these species, even though their geometries are largely unaffected by solvation.

Table 1. Dissociation and reduction free energies (kcal mol^{-1}) computed with and without the inclusion of rovibrational corrections in free energies of solvation, and the corresponding deviations with respect to experimental p*K*as and reduction potentials.

Solvent	dataset	$\Delta\Delta G^{*\,a}_{soln}$	RMSD	Δ_{expt} (eqn 1)^{b,d}	Δ_{expt} (eqn 4)^{c,d}
Water	83 p*K*as	0.45 (2.00)	0.44	4.42	4.59
DMSO	34 p*K*as	0.40 (1.79)	0.34	2.59	2.53
Water	42 E^o	0.34 (1.09)	0.26	0.24	0.25

[a] The mean absolute value of eqn (9) (in kcal mol^{-1}) evaluated at the M06-2X/6-31+G(d) level of theory. Maximum absolute deviations are shown in parenthesis. [b] Mean absolute deviation from experimental p*K*as (pH units) and reduction potentials (in electron volts) using the cycles shown in Figure 1 and free energies of solvation from eqn (1) at the M06-2X/6-31+G(d) level of theory. [c] Mean absolute deviation from experimental p*K*as (pH units) and reduction potentials (in electron volts) using the cycles shown in Figure 1 and free energies of solvation from eqn (4) at the M06-2X/6-31+G(d) level of theory. [d] The gas phase energies were computed at G3(MP2)-RAD(+)//M06-2X/6-31+G(d) level of theory.

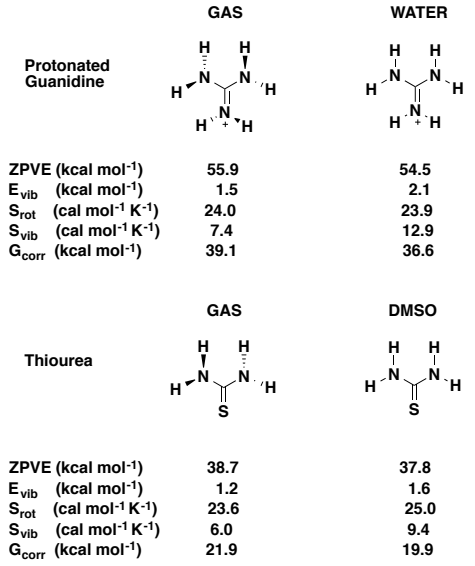

Figure 2. The gas phase and solution phase geometries of protonated guanidine and thiourea. The rotational and vibrational contributions to the thermal correction in each phase are also shown.

The mean absolute deviation associated with calculated p*K*as and reduction potentials with experiment are shown in the last two columns of Table 1. Overall, it appears that including vibrational corrections in free energies of solvation does not affect the results appreciably, where the mean absolute error in p*K*as and reduction potentials calculated by the two approaches are within 0.2 units and 10 mV of each other respectively. Interestingly, including vibrational corrections in the free energy of solvation increased the error for protonated guanidine by 1.5 p*K*a units, whereas the p*K*a for thiourea is improved by the same degree. For the aliphatic alcohols, the error increased by about 1.3 units in all cases. Table 2 lists the free energies of solvation for several solutes for which experimental values are available. It is interesting to note that including vibrational corrections (amounting to 1-2 kcal mol^{-1}) did not improve the agreement with experimental free energies of solvation. It is important to point out that for selected ionic solutes, the SMD solvation model has been parameterised to reproduce the solvation free energies of their hydrated clusters rather than the *bare* ions.[18] As noted in an earlier study,[44] the vibrational contributions to the free energy of solvation are significantly smaller when these solutes are clustered, which are consistent with the results for the methoxide and ethoxide anions shown in Table 2.

Table 2. Fixed concentration free energies of solvation (kcal mol^{-1})^a for selected solutes displaying large vibrational contributions.

	Expt	$\Delta G^{*\,b}_S$	ΔG^{*}_S(vib) ^{c}
Guanidinium(+)	-66.1[61]	-69.1	-71.5
Urea	-13.8[18]	-14.8	-15.7
CH_3O(-)	-95.2[62]	-83.5	-81.8
CH_3CH_2O(-)	-91.1[62]	-80.1	-78.7
$CH_3O(H_2O)$(-)	-80.1[18]	-75.6	-74.6
$CH_3CH_2(H_2O)$(-)	-78.5[18]	-73.7	-73.2

[a] Computed at the M06-2X/6-31+G(d) level. [b] Computed using eqn (1). [c] Computed using eqn (4).

In the present study, we find that the rotational contribution to the free energies of solvation is generally very small (< 0.1 kcal mol^{-1}). As noted elsewhere,[44] this is due to the dependence of the (unhindered) rotational partition function on the molecular principal moments of inertia, which makes them generally very insensitive to the small changes in geometry associated with solvation. The makeover of the gas phase rotational modes to librational modes in the solution phase is also implicitly included in the parameterisation of the non-electrostatic terms in the SMD model.[44] As such, the present results indicate that the rotational contribution based on the gas phase rigid rotor partition function is negligibly small that it should not introduce significant errors. Interestingly, the use of vibrationally-corrected free energies of solvation (when these effects are significant, i.e. > 1.4 kcal mol^{-1}) does not necessarily improve the quality of the free energy of solvation or p*K*as. The data presented in Table 2 indicates that this might be due to the increased error in the calculated free energies of solvation when vibrational corrections are included, though further studies are necessary to investigate the generality of this finding. Nevertheless, when solvation induced changes in the geometry and frequencies are small, accounting for rovibrational contributions in free energies of solvation has negligible impact on computed p*K*as and reduction potentials.

4.2 High level calculations in the gas phase or continuum?

As noted before, one can improve the accuracy of solution phase free energies obtained from a thermodynamic cycle by performing the gas phase calculations at a higher level of theory (eqn (8)). An alternative approach is to perform all calculations directly within the continuum model (eqn (10)), and this section

examines the p*K*as and reduction potentials calculated using the two procedures.

Table 3 compares both approaches against the calculation of 143 dissociation free energies in water, DMSO and acetonitrile and 42 aqueous reduction free energies. The (RO)MP2/GTMP2Large and G3(MP2)-RAD(+) single point calculations in eqn (8) were performed on the M06-2X/6-31+G(d) *gas phase* optimised geometries whereas the corresponding calculations in eqn (10) were carried out on *solution phase* optimised geometries, so that the deviation between the two sets of dissociation free energies is directly quantified by eqn (11). As seen in Table 3, this difference is generally very small, where the mean absolute differences are consistently within 0.8 kcal mol^{-1} for the various solvents (see column 3 and 6 of Table 3), and that the overall MAD is ca. 0.5 kcal mol^{-1} for the MP2/GTMP2Large and G3(MP2)-RAD(+) calculations. The complete data is provided in Tables S2-S4 in the Supporting Information.

Overall, it appears that the deviation between both approaches is slightly smaller when the high-level single-point calculation is carried out at the G3(MP2)-RAD(+) level. In particular, the number of occurrences (*n*) where the deviation exceeds 1.4 kcal mol^{-1} (corresponding to 1 p*K*a unit) is 3 times higher at the MP2/GTMP2Large level. It is interesting to note that the systems displaying the highest deviation at the G3(MP2)-RAD(+) level are dissociation of ammonia (1.9 kcal mol^{-1}) and water (1.3 kcal mol^{-1}), and the reduction of p-cyano-aniline radical cation and α-hydroxy-alkoxy radicals (1.6 kcal mol^{-1}) in aqueous solution. This observation is surprising in light of the size of some of these systems, and that their geometries are mostly unaffected by solvation. By comparison, the deviations are 1.1. and 0.3 kcal mol^{-1} for guanidinium (in water) and thiourea (in DMSO) that undergo more pronounced geometrical changes upon solvation. For ammonia and water, the deviation failed to improve even when the high level single point calculation is performed at the CCSD(T)/aug-cc-pV5Z. It is also interesting to note that other similar-sized species (e.g. hydrogen fluoride, hydrogen peroxide and hydrogen sulphide) display deviations that are significantly smaller. For these systems, it appears that there is no systematic correlation between the magnitude of the deviation $\Delta\Delta G^{*}_{soln}$ (eqn (11)) and the level of theory, or geometrical changes associated with solvation.

Table 4 compares the aqueous p*K*as computed via the two approaches with experiment. The results have been further categorised according to the functionality of the solutes. In the column under "M06-2X/6-31+G(d)", both gas phase and solvation free energies in the thermodynamic cycle are computed at this level of theory (i.e. L=H in eqn (8)), so that both the thermodynamic cycle and direct approaches yield identical results. Table 5 shows the corresponding results for the aqueous reduction potentials. Consistent with the results presented in Table 3, both thermodynamic cycle and direct approach yield very similar p*K*as and reduction potentials for the various classes of compounds. Notably, the *difference* in the overall mean absolute deviation (MAD) with experiment is within 0.15 p*K*a units when the reaction energies were corrected at the MP2/GTMP2Large and G3(MP2)-RAD(+) levels. For example, the mean absolute deviation in the thermodynamic cycle and direct approaches are 3.52 and 3.59 respectively (last row of Table 4). Similarly, the difference is less than 10 mV for the calculated reduction potentials. For both approaches, the overall mean absolute deviations with experiment in the computed p*K*as and reduction potentials are about 3.5 units and 250 mV, which are consistent with results from recent assessment studies.[10, 11, 27, 63]

It is interesting to note from Tables 4 and 5 that the use of high-level ab initio calculations did not necessarily improve the average accuracy of the resulting solution phase energies in both thermodynamic cycle and direct methods. For example, the MAD is reduced from 3.9 to about 1.4 units for carboxylic acids when the reaction energies were computed at the G3(MP2)-RAD(+) level of theory compared to those computed at the M06-2X/6-31+G(d) level (see second row of Table 4). However, the MAD increased by 2.8 units for alcohols. For the thermodynamic cycle approach, this indicates that there is likely to be some degree of error cancellation when the solution phase reaction energy is obtained from adding gas phase and solvation terms such that improving the accuracy of individual contributions can sometimes worsen the accuracy of the resulting reaction energy.

Table 3. Mean absolute difference (kcal mol^{-1}) between dissociation free energies computed via the thermodynamic cycle and directly within the SMD continuum model.

		MP2[a]			G3[b]		
Solvent	*N*[c]	MAD	AD_{max}	*n*[d]	MAD	AD_{max}	*n*[d]
Water	83 p*K*as	0.64	2.29	5	0.53	1.86	1
Dimethylsulfoxide	30 p*K*as	0.39	1.63	1	0.35	0.99	0
Acetonitrile	30 p*K*as	0.39	1.42	1	0.36	0.93	0
Water	42 *E*°	0.76	2.30	6	0.64	1.57	3
Overall	143	0.54	2.29	13	0.46	1.87	4

[a] Computed using eqn (10) where H = MP2/GTMP2Large and L = M06-2X/6-31+G(d). [b] Computed using eqn (10) where H =G3(MP2)-RAD(+) and L = M06-2X/6-31+G(d). [c] Size of the dataset. [d] Number of occurrences where the deviation is larger than 1.4 kcal mol^{-1}.

Table 4. Comparison of calculated aqueous p*K*as[a] via the thermodynamic cycle and direct approach with experiment.

solutes	*N*[b]	M06-2X/6-31+G(d)[c]		MP2-TC[d]		MP2-Direct[e]		G3-TC[f]		G3-Direct[g]	
		MAD	AD_{max}	MAD	AD_{max}	MAD	AD_{max}	MAD	AD_{max}	MAD	AD_{max}
Alcohols	13	3.04	6.43	3.78	7.7	4.00	8.0	5.70	9.64	5.80	9.91
Carboxylic acids	7	3.88	6.88	2.41	4.46	2.41	4.46	1.30	2.38	1.49	2.73
Inorganic acids	14	4.91	10.25	5.02	8.04	5.17	7.69	4.63	10.35	4.82	9.79
Carbon acids	21	2.97	5.25	3.22	6.96	3.44	6.55	4.47	6.98	4.72	6.84
Cationic acids	28	3.67	7.71	3.15	6.11	3.02	6.44	2.63	6.06	2.64	5.98
Overall	83	3.62	10.25	3.52	8.04	3.59	7.99	3.80	10.35	3.93	9.91

[a] Using the thermodynamic cycle A shown in Figure 1. All geometries and thermal corrections are obtained at the M06-2X/6-31+G(d) level of theory. [b] Size of the dataset. [c] Gas phase energies computed at M06-2X/6-31+G(d) level of theory. Both thermodynamic cycle and direct approach yields identical results. [d] Gas phase energies were corrected by a MP2/GTMP2Large single-point calculation – eqn (8). [e] Solution phase energies were corrected by a MP2/GTMP2Large single-point calculation in the SMD model – eqn (9). [f] Gas phase energies were corrected by a G3(MP2)-RAD(+) composite calculation – eqn (8). [g] Solution phase energies were corrected by a G3(MP2)-RAD(+) composite calculation in the SMD model – eqn (9).

Table 5. Comparison of calculated aqueous reduction potentials[a] via the thermodynamic cycle and direct approach with experiment.

Solutes		M06-2X/6-31+G(d)[c]		MP2-TC[d]		MP2-Direct[e]		G3-TC[f]		G3-Direct[g]	
	N[b]	MAD	AD_{max}	MAD	AD_{max}	MAD	AD_{max}	MAD	AD_{max}	MAD	AD_{max}
Amines	14	0.18	0.37	0.17	0.31	0.19	0.38	0.09	0.21	0.10	0.26
Nitroxides	4	0.12	0.14	0.08	0.13	0.11	0.16	0.15	0.19	0.10	0.15
Alcohols	24	0.24	0.47	0.29	0.64	0.30	0.63	0.36	0.68	0.36	0.67
Overall	42	0.21	0.47	0.23	0.64	0.24	0.63	0.25	0.68	0.25	0.67

[a] Using the thermodynamic cycle B shown in Figure 1. All geometries and thermal corrections are obtained at the M06-2X/6-31+G(d) level of theory. [b] Size of the dataset. [c] Gas phase energies computed at M06-2X/6-31+G(d) level of theory. Both thermodynamic cycle and direct approach yields identical results. [d] Gas phase energies were corrected by a (RO)MP2/GTMP2Large single-point calculation – eqn (8). [e] Solution phase energies were corrected by a (RO)MP2/GTMP2Large single-point calculation in the SMD model – eqn (9). [f] Gas phase energies were corrected by a G3(MP2)-RAD(+) composite calculation – eqn (8). [g] Solution phase energies were corrected by a G3(MP2)-RAD(+) composite calculation in the SMD model – eqn (9).

4.3 What is the source of agreement between direct and thermodynamic cycle approaches?

The above results raises the question as to why direct calculation of reaction free energies in the SMD continuum model does not circumvent the errors encountered in thermodynamic cycle based methods. As noted before, the deviation in the reaction energy computed via the two approaches is quantified by difference in the high level correction to the reaction energy computed in the gas phase and SMD model on geometries optimised in the respective phases – eqn (11). It seems reasonable that for small to medium-sized solutes where solvation induced changes in structure are usually small that the deviation between direct and thermodynamic cycle approaches is generally small. Alternatively, rearrangement of eqn (11) in terms of solvation free energies defined by eqn (1) shows that the deviation in the dissociation energies from the two approaches is directly related to the difference in the solvation contribution ($\Delta\Delta G^*_S$) to the dissociation/reduction free energy computed at the high (X=H) and low (X=L) levels of theory.

$$\Delta\Delta G^*_{soln} = \Delta G^*_{soln}(\mathrm{TC}) - \Delta G^*_{soln}(\mathrm{direct}) \quad (12a)$$

$$\Delta\Delta G^*_{soln} = \Delta\Delta G^*_S(\mathrm{L}) - \Delta\Delta G^*_S(\mathrm{H}) \quad (12b)$$

$$\Delta\Delta G^*_S(\mathrm{X}) = [\Delta G^*_S(\mathrm{A}^-) - \Delta G^*_S(\mathrm{HA})]_X \quad (12c)$$

In this context, the agreement between direct and thermodynamic cycle approaches also indicates that the solvation contribution calculated by the SMD model is relatively insensitive to the choice of electronic structure method. This is presumably a reflection of the semi-empirical nature of continuum solvation models.

We have further investigated cases where solvation induced changes in geometries are significant. For example, amino acids exist as two different tautomers in the gas and solution phase, and that the solution phase zwitterionic tautomer is not a stationary point on the gas phase potential energy surface.[64-66] Shown in Table 6 are the first and second p*K*as of a series of amino acids calculated via the thermodynamic cycle (Figure 1) and directly within the SMD model. We found for these systems, that direct calculation of dissociation free energies within the continuum model yields p*K*as that are in better agreement with experiment, where the MAD is approximately 1 unit less than that of the cycle approach. The improvement afforded by the direct approach is consistent with expectation since the high-level correction to the reaction energy is being carried out on the actual active solution phase species. As such, direct calculation of free energy changes in the SMD continuum model generally yields very similar results to thermodynamic cycles when solvation induced changes in geometries are small. Where this is not the case, the direct approach appears to perform better than the thermodynamic cycle approach since the higher level

electronic structure calculations are carried out on the solution phase species.

Table 6. The first and second dissociation constants of common amino acids calculated directly within the SMD continuum model and via a thermodynamic cycle.

	p*K*a1			p*K*a2		
	Direct[a]	TC[b]	Expt[67]	Direct[a]	TC[b]	Expt[67]
Glycine	2.89	2.54	2.34	10.71	10.27	9.58
Alanine	3.16	1.03	2.33	10.89	12.18	9.71
Valine	3.18	1.07	2.27	11.27	12.35	9.52
Leucine	3.10	0.99	2.32	11.31	12.46	9.58
Serine	1.85	-0.40	2.13	10.47	11.62	9.05
Cysteine	1.76	0.18	1.91	11.54	12.89	10.28
Proline	2.33	0.73	1.95	12.78	13.61	10.47
Methionine	2.20	1.12	2.16	11.22	12.15	9.08
MAD	0.49	1.32		1.62	2.53	

[a] Calculated directly within the SMD continuum model eqn (10) where H=G3(MP2)-RAD(+) and L=M06-2X/6-31+G(d). [b] Calculated using the thermodynamic cycle A in Figure 1 eqn (8) where H=G3(MP2)-RAD(+) and L=M06-2X/6-31+G(d).

5. Conclusions

We have examined several pertinent issues concerning continuum solvent calculation of solution phase p*K*as and reduction potentials. We found that including vibrational corrections in the SMD free energies of solvation generally has a very small effect (within 0.5 kcal mol^{-1}) on the reaction energies calculated via the cycle approach for the small to medium-sized systems examined in this study. The contribution becomes non-negligible (~1-2 kcal mol^{-1}) for systems where solvation induced changes in geometry and/or vibrational frequencies are significant. However, for the systems examined in this study, including vibrational corrections in the free energies of solvation did not necessarily improve accuracy. Further studies are necessary to establish the generality of these findings.

Additionally, we compared the accuracy of p*K*as and reduction potentials calculated directly within the SMD dielectric continuum model, and via a thermodynamic cycle against the calculation of 117 p*K*as and 42 reduction potentials in water and DMSO encompassing a broad range of species. The study showed that both approaches generally give very similar results (0.5 kcal mol^{-1} or 0.4 p*K*a unit) which is well within the mean accuracy of the p*K*a and redox potential calculation protocols. We reasoned that the source of agreement is due to the relatively small change in geometries associated with solvation displayed by the solutes in the test set. We further demonstrated for amino acids where the solution phase geometries differ appreciably from the gas phase, that carrying out high-level single-point calculations directly in the continuum model on the solution phase species give rise to p*K*as that are in better agreement with experiment.

Accordingly, the present results indicates that direct calculation of free energies in the SMD model, at least in the case of p*K*as and reduction potentials, is generally a reliable approximation to corresponding thermodynamic cycle calculations. Additionally, when solution phase structure differs appreciably from the gas phase, the direct approach is shown to provide improvement compared to the thermodynamic cycle calculations presumably because the high-level energy corrections are focused on the actual solution phase species involved in the dissociation process. It is of interest to examine the generality of these results with respect to the calculation of reaction barriers, as well as for other continuum solvation models, which we are currently investigating.

Acknowledgements

The author acknowledges support from the Agency for Science and Technology, and the A*STAR Computational Resource Centre (ACRC) and Yale High Performance Computing facility for generous allocation of computing time.

Notes and references

[a] Department of Chemistry, Yale University, 225 Prospect Street, New Haven CT 06520, United States. [b] Institute of High Performance Computing, Agency for Science, Technology and Research, 1 Fusionopolis Way, #16-16, Connexis, Singapore 138632. junming.ho@yale.edu

Electronic Supplementary Information (ESI) available: G3(MP2)-RAD(+) electronic energies, SMD free energies of solvation, computed and experimental p*K*as and reduction potentials of dataset of molecules. See DOI: 10.1039/b000000x/

1. J. Tomasi, B. Mennucci and R. Cammi, *Chem. Rev.*, 2005, 105, 2999-3093.
2. C. J. Cramer and D. G. Truhlar, *Chem. Rev.* , 1999, 99, 2161-2200.
3. D. Bashford and D. A. Case, *Annu. Rev. Phys. Chem.*, 2000, 51, 129-152.
4. M. Orozco and F. J. Luque, *Chem. Rev.*, 2000, 100, 4187-4225.
5. See for example (a) C. Y. Lin, E. I. Izgorodina and M. L. Coote, *Macromolecules*, 2010, **43**, 553-560. (b) J. D. Modglin, J. C. Dunham, C. W. Gibson, C. Y. Lin, M. L. Coote and J. S. Poole, *J. Phys. Chem. A*, 2011, **115**, 2431-2441 (c) B. B. Noble and M. L. Coote, *Int. Rev. in Phys. Chem.*, 2013, **32**, 467-513. (d) I. Degirmenci, T. F. Ozaltin, O. Karahan, V. van Speybroeck, M. Waroquier and V. Aviyente, *Polymer Chem.*, 2013, **51**, 2024-2034.
6. See for example (a) D. M. Chipman, *J. Phys. Chem. A,* 2002, **106**, 7413-7422. (b) J. J. Klicic, R. A. Friesner, S.-Y. Liu and W. C. Guida, *J. Phys. Chem. A* 2002, **106**, 1327-1335. (c) J. R. Pliego, Jr. and J. M. Riveros, *J. Phys. Chem. A* 2002, **106**, 7434-7439. (d) A. M. Magill, K. J. Cavell and B. F. Yates, *J. Am. Chem. Soc.*, 2004, **126**, 8717-8724. (e) Y. Fu, L. Liu, R.-Q. Li, R. Liu and Q.-X. Guo, *J. Am. Chem. Soc.*, 2004, **126**, 814-822. (f) C. P. Kelly, C. J. Cramer and D. G. Truhlar, *J. Phys. Chem. A*, 2006, **110**,

2493-2499 (g) M. Namazian, M. Zakery, M. R. Noorbala and M. L. Coote, *Chem. Phys. Lett.*, 2008, **451**, 163-168. (h) E. F. da Silva, H. F. Svendsen and K. M. Merz, *J. Phys. Chem. A*, 2009, **113**, 6404-6409. (i) J. Ho, M. L. Coote, M. Franco-Perez and R. Gomez-Balderas, *J. Phys. Chem. A*, 2010, **114**, 11992-12003 (j) J. A. Keith and E. A. Carter, *J. Chem. Theory and Comput.*, 2012, **8**, 3187-3206. (k) E. L. M. Miguel, P. L. Silva and J. R. J. Pliego, *J. Phys. Chem. B*, 2014, **118**, 5730-5739

7. See for example (a) M. H. Baik and R. A. Friesner, *J. Phys. Chem. A* 2002, **106**, 7407-7412. (b) P. Winget, C. J. Cramer and D. G. Truhlar, *Theor. Chem. Acc.*, 2004, **112**, 217 (c) Y. Fu, L. Liu, H.-Z. Yu, Y.-M. Wang and Q.-X. Guo, *J. Am. Chem. Soc.*, 2005, **127**, 7227-7234. (d) M. Schmidt am Busch and E.-W. Knapp, *J. Am. Chem. Soc.*, 2005, **127**, 15730-15737 (e) P. Jaque, A. V. Marenich, C. J. Cramer and D. G. Truhlar, *J. Phys. Chem. C* 2007, **111**, 5783-5799 (f) A. S. Dutton, J. M. Fukuto and K. N. Houk, *Inorg. Chem.*, 2005, **44**, 4024-4028 (g) J. L. Hodgson, M. Namazian, S. E. Bottle and M. L. Coote, *J. Phys. Chem. A*, 2007, **111**, 13595-13605 (h) L. E. Roy, E. Jakubikova, M. G. Guthrie and E. R. Batista, *J. Phys. Chem. A*, 2009, **113**, 6745-6750. (i) G. Gryn'ova, J. M. Barakat, J. P. Blinco, S. E. Bottle and M. L. Coote, *Chem. Eur. J.*, 2012, **18**, 7582-7593. (j) A. V. Marenich, A. Majumdar, M. Lenz, C. J. Cramer and D. G. Truhlar, *Angew. Chem. Intl. Ed.*, 2012, **51**, 12810-12814. (k) B. T. Psciuk and B. H. Schlegel, *J. Phys. Chem. B*, 2013, **117**, 9518-9531.
8. G. C. Shields and P. G. Seybold, *Computational Approaches for the Prediction of pKa Values*, CRC Press, 2013.
9. K. S. Alongi and G. C. Shields, *Annu. Rep. Comput. Chem.*, 2010, 6, 113-138.
10. A. V. Marenich, J. Ho, M. L. Coote, C. J. Cramer and D. G. Truhlar, *Phys. Chem. Chem. Phys.*, 2014, **16**, 15068-15106.
11. J. Ho and M. L. Coote, *Theor. Chem. Acc.*, 2010, **125**, 3-21.
12. J. Ho and M. L. Coote, *Comput. Mol. Sci.*, 2011, **1**, 649.
13. J. Tomasi, B. Mennucci and E. Cances, *J. Mol. Structure: (THEOCHEM)*, 1999, **464**, 211-226.
14. V. Barone and M. Cossi, *J. Phys. Chem. A* 1998, **102**, 1995-2001.
15. A. Klamt and G. Schurmann, *J. Chem. Soc., Perkin Trans. 2* , 1993, 799-805.
16. J. B. Foresman, T. A. Keith, K. B. Wiberg, J. Snoonian and M. J. Frisch, *J. Phys. Chem.* , 1996, **100**, 16098-16104.
17. A. V. Marenich, R. M. Olson, C. P. Kelly, C. J. Cramer and D. G. Truhlar, *J. Chem. Theor. Comput.*, 2007, **3**, 2011-2033.
18. A. V. Marenich, C. J. Cramer and D. G. Truhlar, *J. Phys. Chem. B*, 2009, **113**, 6378-6396.
19. C. Curutchet, A. Bidon-Chanal, I. Soteras, M. Orozco and F. J. Luque, *J. Phys. Chem. B*, 2005, **109**, 3565.
20. C. Curutchet, M. Orozco and F. J. Luque, *J. Comput. Chem.*, 2001, **22**, 1180.
21. D. M. Chipman, *J. Chem. Phys.*, 2000, **112**, 5558-5565.
22. D. M. Chipman, *J. Chem. Phys.*, 1999, **110**, 8012-8018.
23. B. Marten, K. Kim, C. Cortis, R. A. Friesner, R. B. Murphy, M. Ringnalda, D. Sitkoff and B. Honig, *J. Phys. Chem.*, 1996, **100**, 11775-11788.
24. A. Klamt, *Comp. Mol. Sci.*, 2011, **1**, 699-709.
25. A. Klamt, *COSMO-RS: From Quantum Chemistry to Fluid Phase Thermodynamics and Drug Design*, Elsevier Science Ltd., Amsterdam, The Netherlands, 2005.
26. A. Klamt, V. Jonas, T. Burger and J. C. W. Lohrenz, *J. Phys. Chem. A*, 1998, **102**, 5074-5085.
27. J. J. Guerard and J. S. Arey, *J. Chem. Theory and Comput.*, 2013, **9**, 5046-5058.
28. C. J. Cramer and D. G. Truhlar, *Acc. Chem. Res.*, 2008, **41**, 760-768.
29. A. Klamt, B. Mennucci, J. Tomasi, V. Barone, C. Curutchet, M. Orozco and F. J. Luque, *Acc. Chem. Res.*, 2009, **42**, 489-492.
30. J. Ho, *Aust. J. Chem.*, 2014,67, 1441-1460
31. D. Asthagiri, L. Pratt and H. S. Ashbaugh, *J. Chem. Phys.*, 2003, **119**, 2702-2708.
32. S. B. Rempe, L. R. Pratt, G. Hummer, J. D. Kress, R. L. Martin and A. Redondo, *J. Am. Chem. Soc.*, 2000, **122**, 966-967.
33. J. R. Pliego, Jr. and J. M. Riveros, *J. Phys. Chem. A* 2001, **105**, 7241-7247.
34. D. Himmel, S. K. Goll, I. Leito and I. Krossing, *Chem. Eur. J.*, 2011, **17**, 5808-5826.
35. V. S. Bryantsev, M. S. Diallo and W. A. Goddard III, *J. Phys. Chem. B*, 2008, **112**, 9709-9719.
36. G. J. Tawa, I. A. Topol, S. K. Burt, R. A. Caldwell and A. A. Rashin, *J. Chem. Phys.*, 1998, **109**, 4852.
37. T. N. Brown and N. Mora-Diez, *J. Phys. Chem. B*, 2006, **110**, 9270-9279.
38. T. N. Brown and N. Mora-Diez, *J. Phys. Chem. B*, 2006, **110**, 20546-20554.
39. K. K. Govender and I. Cukrowski, *J. Phys. Chem. A*, 2010, **114**, 1868-1878.
40. K. K. Govender and I. Cukrowski, *J. Phys. Chem. A*, 2009 **113**, 3639-3647.
41. J. L. Pruszynski and S. D. Wetmore, *J. Phys. Chem. B*, 2009, **113**, 6533-6542.
42. J. Ho, A. Klamt and M. L. Coote, *J. Phys. Chem. A*, 2010, **114**, 13442-13444.
43. A. Ben-Naim, in *Statistical Thermodynamics for Chemists and Biochemists*, Plenum, New York, 1992, p. 321.
44. R. F. Ribeiro, A. V. Marenich, C. J. Cramer and D. G. Truhlar, *J. Phys. Chem. B*, 2011, **115**, 14556-14562.
45. S. Sastre, R. Casanovas, F. Munoz and J. Frau, *Theor. Chem. Acc.*, 2013, **132**, 1310.
46. R. Casanovas, D. Fernandez, J. Ortega-Castro, J. Frau, J. Donoso and F. Munoz, *Theor. Chem. Acc.*, 2011, **130**, 1-13.
47. R. Casanovas, J. Ortega-Castro, J. Donoso, J. Frau and F. Munoz, *Phys. Chem. Chem. Phys.*, 2013, **15**, 16303-16313.
48. R. Casasnovas, J. Ortega-Castro, J. Frau, J. Donoso and F. Munoz, *Int. J. Quantum. Chem.*, 2014, **114**, 1350-1363.
49. D. G. Truhlar, B. C. Garrett and S. J. Klippenstein, *J. Phys. Chem.*, 1996, **100**, 12771-12800.
50. Gaussian 09 Revision D.01, Frisch, M. J.; Trucks, G. W.; Schlegel, H. B.; Scuseria, G. E.; Robb, M. A.; Cheeseman, J. R.; Scalmani, G.; Barone, V.; Mennucci, B.; Petersson, G. A.; Nakatsuji, H.; Caricato, M.; Li, X.; Hratchian, H. P.; Izmaylov, A. F.; Bloino, J.; Zheng, G.; Sonnenberg, J. L.; Hada, M.; Ehara, M.;

Toyota, K.; Fukuda, R.; Hasegawa, J.; Ishida, M.; Nakajima, T.; Honda, Y.; Kitao, O.; Nakai, H.; Vreven, T.; Montgomery, Jr., J. A.; Peralta, J. E.; Ogliaro, F.; Bearpark, M.; Heyd, J. J.; Brothers, E.; Kudin, K. N.; Staroverov, V. N.; Kobayashi, R.; Normand, J.; Raghavachari, K.; Rendell, A.; Burant, J. C.; Iyengar, S. S.; Tomasi, J.; Cossi, M.; Rega, N.; Millam, N. J.; Klene, M.; Knox, J. E.; Cross, J. B.; Bakken, V.; Adamo, C.; Jaramillo, J.; Gomperts, R.; Stratmann, R. E.; Yazyev, O.; Austin, A. J.; Cammi, R.; Pomelli, C.; Ochterski, J. W.; Martin, R. L.; Morokuma, K.; Zakrzewski, V. G.; Voth, G. A.; Salvador, P.; Dannenberg, J. J.; Dapprich, S.; Daniels, A. D.; Farkas, Ö.; Foresman, J. B.; Ortiz, J. V.; Cioslowski, J.; Fox, D. J. Gaussian, Inc., Wallingford CT, 2009.

51. F. Ding, J. M. Smith and H. Wang, *J. Org. Chem.*, 2009, **74**, 2679-2691.
52. Y. Zhao and D. G. Truhlar, *Theor. Chem. Acc.* , 2008, **120**, 215-241.
53. D. J. Henry, M. B. Sullivan and L. Radom, *J. Chem. Phys.*, 2003, **118**, 4849-4860.
54. C. P. Kelly, C. J. Cramer and D. G. Truhlar, *J. Phys. Chem. B* 2006, **110**, 16066-16081.
55. M. D. Tissandier, K. A. Cowen, W. Y. Feng, E. Gundlach, M. H. Cohen, A. D. Earhart, J. V. Coe and T. R. Tuttle, Jr., *J. Phys. Chem. A* 1998, **102**, 7787-7794.
56. C. P. Kelly, C. J. Cramer and D. G. Truhlar, *J. Phys. Chem. B* 2007, **111**, 408-422.
57. A. Moser, K. Range and D. M. York, *J. Phys. Chem. B*, 2010, **114**, 13911-13921.
58. J. E. Bartmess, *J. Phys. Chem.*, 1994, **98**, 6420-6424.
59. J. Ho, M. L. Coote, C. J. Cramer and D. G. Truhlar, in *Organic Electrochemistry*, eds. O. Hammerich and B. Speiser, 2015 (in press).
60. A. A. Isse and A. Gennaro, *J. Phys. Chem. B*, 2010, **114**, 7894-7899.
61. M. M. Reif, P. H. Hünenberger and C. Oostenbrink, *J. Chem. Theory and Comput.*, 2012, **8**, 3705-3723.
62. J. R. Pliego, Jr. and J. M. Riveros, *Phys. Chem. Chem. Phys.* , 2002, **4**, 1622-1627.
63. J. Ho and M. L. Coote, *J. Chem. Theory Comput.*, 2009, **5**, 295-306.
64. M. S. Gordon and J. H. Jensen, *Acc. Chem. Res.*, 1996, **29**, 536-543.
65. J. H. Jensen and M. S. Gordon, *J. Am. Chem. Soc.*, 1995, **117**, 8159-8170.
66. D. Yu, D. A. Armstrong and A. Rauk, *Can. J. Chem.*, 1992, **70**, 1762.
67. "Physical Constants of Organic Compounds", in CRC Handbook of Chemistry and Physics, Internet Version 2005, David R. Lide, ed., <http://www.hbcpnetbase.com>, CRC Press, Boca Raton, FL 2005.